THERMOACOUSTICS MODELING OF LOUDSPEAKERS WITH COMSOL MULTIPHYSICS

Patrick Grahn

COMSOL Oy
Arabiankatu 12
00560 Helsinki
patrick@comsol.fi

Abstract

Thermal conduction and viscous losses are important considerations when modeling the acoustic performance of small-scale audio equipment, such as hearing aids, cell phones and loudspeaker drivers. Introducing thermoacoustic effects into a simulation properly accounts for these frequency-dependent losses. In this presentation, we review the theoretical principle of thermoviscous acoustics and demonstrate its application by using a simulation model of a loudspeaker. Simulations are performed using the acoustics module of COMSOL Multiphysics.

1 INTRODUCTION

Finite element simulations using COMSOL Multiphysics are often used for the design and product development of loudspeaker drivers [1-8]. From these simulations one can derive important loudspeaker characteristics, such as sensitivity, directivity and energy efficiency. It is then straightforward to investigate how decisions on the loudspeaker geometry and materials affect the acoustic performance. Ultimately, this results in a decreased need for physical prototypes.

Acoustic simulation software typically solve the Helmholtz equation in the fluid domains. This inherently assumes an adiabatic development of the acoustic quantities, which neglects thermal and viscous boundary effects. However, when modeling small-scale audio devices, this assumption can no longer be made and the solution of Helmholtz equation provides erroneous results. Instead, it is necessary to consider a thermoacoustics formulation, based on the linearized Navier-Stokes equation. Such a formulation is provided by COMSOL's thermoacoustics interface, included in the acoustics module.

In this paper, we present the theory of thermoacoustics that is necessary for viscothermal modeling of miniature loudspeakers. We also create a COMSOL model of a balanced armature receiver, which is a typical loudspeaker used for in-ear headphones, hearing instruments and security headsets. We solve the model using thermoacoustics and analyze the results. These results are then compared to those obtained with lossless pressure acoustics that solve the Helmholtz equation.

2 MATHEMATICAL DESCRIPTION

Acoustic waves are small harmonic variations of pressure in a fluid, which are superposed on a background pressure. The fundamental equations governing these waves can be obtained by linearizing the Navier-Stokes equation, continuity equation and energy equation. In frequency domain, the resulting equations can be expressed in a source-free fluid as

$$\mathrm{j}\omega\rho_0\mathbf{u} = -\nabla p + \nabla\cdot\left(\mu[\nabla\mathbf{u} + (\nabla\mathbf{u})^{\mathrm{T}}] - \left[\frac{2}{3}\mu - \mu_{\mathrm{B}}\right][\nabla\cdot\mathbf{u}]\overleftrightarrow{\mathbf{I}}\right), \tag{1}$$

$$\mathrm{j}\omega\rho + \rho_0\nabla\cdot\mathbf{u} = 0, \tag{2}$$

$$\mathrm{j}\omega\rho_0 C_p T = \nabla\cdot(k\nabla T) + \mathrm{j}\omega p T_0\alpha_0, \tag{3}$$

where ω is the angular frequency and the material parameters ρ_0, μ, μ_{B}, C_p, k and α_0 are the fluid's background density, dynamic viscosity, bulk viscosity, heat capacity at constant pressure, thermal conductivity and isobaric coefficient of thermal expansion, respectively. In the equations, there are four complex-valued quantities that oscillate with the acoustic wave. These are the variations in pressure p, velocity $\mathbf{u}$, temperature T and fluid density ρ. These small-signal quantities are superposed on the background pressure p_0, background temperature T_0 and background density ρ_0. For simplicity, we assume that there is no stationary background velocity field. Thus, the total pressure, velocity, temperature and density as a function of time t can be expressed as follows:

$$p_{\mathrm{tot}}(t) = p_0 + \mathrm{Re}\{pe^{\mathrm{j}\omega t}\}, \tag{4}$$

$$\mathbf{u}_{\mathrm{tot}}(t) = \mathrm{Re}\{\mathbf{u}e^{\mathrm{j}\omega t}\}, \tag{5}$$

$$T_{\mathrm{tot}}(t) = T_0 + \mathrm{Re}\{Te^{\mathrm{j}\omega t}\}, \tag{6}$$

$$\rho_{\mathrm{tot}}(t) = \rho_0 + \mathrm{Re}\{\rho e^{\mathrm{j}\omega t}\}. \tag{7}$$

In addition to Eqs. (1-3), the equation of state

$$\rho = \rho_0(\beta_T p - \alpha_0 T), \tag{8}$$

can be used to substitute the density variation in the continuity equation [Eq. (2)]. This equation requires a seventh material parameter, the isothermal compressibility β_T. Together, equations (1-3) and (8) form the fundamental equations of thermoacoustics, with the three unknowns p, $\mathbf{u}$ and T. These equations can be solved using COMSOL's thermoacoustics interface.

The appearance of thermal and viscous boundary layers is a consequence of the large difference in thermal conductivity and flow properties between fluids and solids. For typical solid-fluid interfaces, it is the case that temperature and velocity variations are zero. This gives rise to a sharp gradient of temperature and velocity near the boundaries, which contributes to Eqs. (1) and (3) through the terms $\nabla\mathbf{u}$, $\nabla\cdot\mathbf{u}$ and ∇T. Note that in the bulk fluid, far from any solid-fluid boundaries, we can neglect the ∇T term in Eq. (3) and combine Eqs. (2), (3) and (8) to obtain

$$\mathrm{j}\omega p + c_s^2\rho_0\nabla\cdot\mathbf{u} = 0, \tag{9}$$

where the speed of sound is defined as

$$c_s = \left(\rho_0 \beta_T - \frac{T_0 \alpha_0^2}{C_p}\right)^{-1/2}. \tag{10}$$

Also the last term in equation (1) disappears far from boundaries. In this case, Equations (1) and (9) can be combined to obtain the Helmholtz equation

$$\nabla^2 p + \frac{\omega^2}{c_s^2} p = 0, \tag{11}$$

which describes a pressure wave in absence of thermoviscous loss. The adiabatic temperature variation and inviscid velocity field are here directly determined by the pressure, through Eqs. (1) and (3) as $\mathbf{u} = \mathrm{j}/(\omega\rho_0)\nabla p$ and $T = T_0\alpha_0/(\rho_0 C_p)p$. In small-scale audio devices, temperature and velocity gradients can be high and Eq. (11) should not be used.

In order to visualize the thermal and viscous boundary layers, let us assume a planar pressure wave propagating in the z-direction in the $x > 0$ half-space. A solid, thermally conducting wall imposes that the acoustic variations $\mathbf{u} = 0$ and $T = 0$ in the $x = 0$ plane. Solving Equations (1-3) and (8) using COMSOL Multiphysics, we obtain the results shown in Figure 1. We can see that there are two transition zones, one where $\mathrm{d}T/\mathrm{d}x \neq 0$ and one where $\mathrm{d}u/\mathrm{d}x \neq 0$. These are the thermal and viscous boundary layers. The extent of these zones can be defined as $2\pi\delta_{\mathrm{therm}}$ and $2\pi\delta_{\mathrm{visc}}$, respectively, where

$$\delta_{\mathrm{therm}} = \left(\frac{2k}{\omega\rho_0 C_p}\right)^{1/2}, \tag{12}$$

$$\delta_{\mathrm{visc}} = \left(\frac{2\mu}{\omega\rho_0}\right)^{1/2}, \tag{13}$$

are defined as the thermal and viscous boundary layer thickness, respectively. Within these layers, the propagation characteristics of acoustic waves are very different compared to the propagation in bulk fluid. Also, thermal and viscous power dissipation occur in these layers. For loudspeaker modeling, the thermoacoustics formulation is necessary in any regions where the physical dimensions are smaller than or comparable to $2\pi\delta_{\mathrm{therm}}$ or $2\pi\delta_{\mathrm{visc}}$.

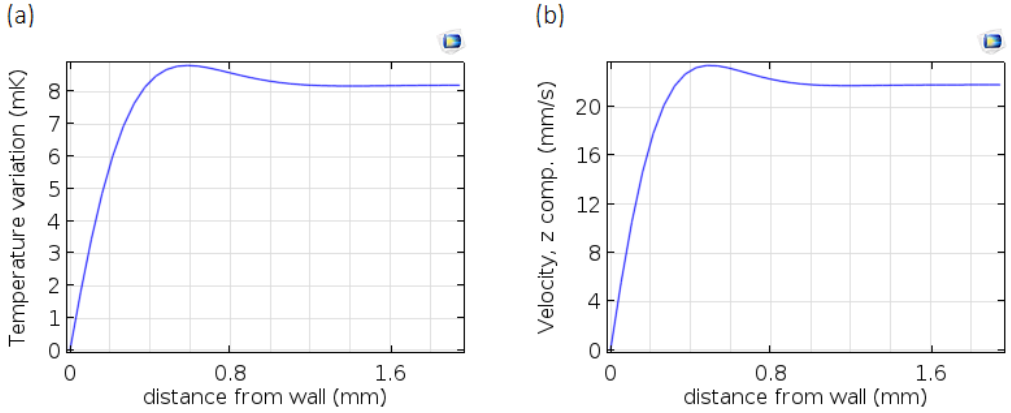

Figure 1. Acoustic temperature and velocity distribution for a plane wave (in air, 20 °C, 1 atm) propagating along a solid wall. A frequency of 100 Hz is used, which corresponds to boundary layer thicknesses of δ_{visc} = 0.22 mm and δ_{therm} = 0.15 mm.

3 LOUDSPEAKER MODEL

As an example of application, we construct a model of a balanced armature receiver. This loudspeaker type is often used in applications where the maximum size and power consumption is limited. Sound pressure levels exceeding well beyond 100 dB can be generated by balanced armature receivers with volumes around 100 mm^3 [9]. However, due to their small sizes, thermal and viscous damping in the system can be significant.

The geometry of a balanced armature receiver, created using COMSOL CAD tools, is shown in Figure 2. The loudspeaker's operating principle is that electrical current in the coil creates a time-dependent magnetic flux in the armature. On the other hand, the armature tip is centered between two equal permanent magnets that create a static magnetic field. Thus, the total force on the armature is the sum of the forces by the permanent magnets and the coil. As the armature starts oscillating, a drive pin connects it mechanically to the diaphragm. The moving diaphragm creates an acoustic pressure wave that leaks out from the front volume via a sound outlet. The pressure wave in the rear volume (the volume containing the coil and magnets), yields a stiffness to the system that impacts the oscillation of the diaphragm. As a consequence, the geometry of the rear volume has a deciding impact on the loudspeaker sensitivity [10].

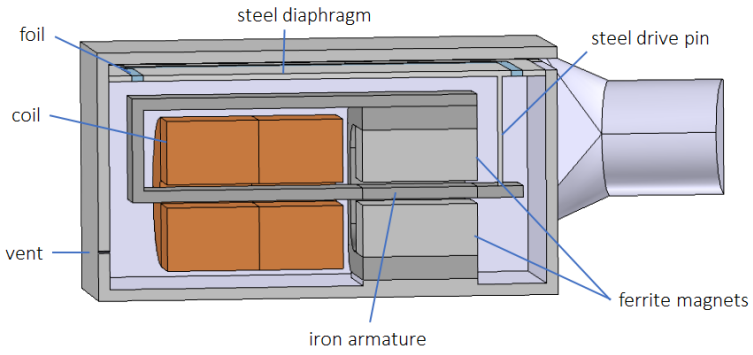

Figure 2. Side view of the balanced armature receiver. Only half of the receiver is drawn, as the structure has reflection symmetry. The vibration of the iron armature is coupled to the diaphragm via a drive pin. The acoustic wave in the front volume goes out through the outlet on the right.

We simulate the acoustic performance of the loudspeaker in the frequency domain. In the model, we solve for acoustics in all air domains, whereas solid mechanics is solved in the armature, pin, diaphragm and foil. The bidirectional coupling between acoustics and mechanics is automatically done in COMSOL, where the solid's acceleration is coupled to the acoustic pressure at the solid-air boundary. It has been shown that a bidirectional coupling is necessary to get a good match with acoustical measurements on real systems [1]. Mechanical damping is added to the diaphragm and foil using an isotropic loss factor of 0.1 and 0.01, respectively.

We use a lumped model to describe the electrical part of the loudspeaker [3]. Neglecting nonlinear effects, the small-signal response is modeled with the electrical circuit shown in Figure 3. The amplitude of the force imposed on the armature is given by the equation

$$F = T_{\mathrm{em}} i, \tag{14}$$

where T_{em} is the force factor. Nonlinear effects could be introduced by adding additional circuit components and terms to Eq. (14) [4]. The force is added to the COMSOL model

as a body load, applied to the part of the armature that is located between the two permanent magnets. A restoring spring force is applied to this same part of the armature, using a spring constant of 600 N/m.

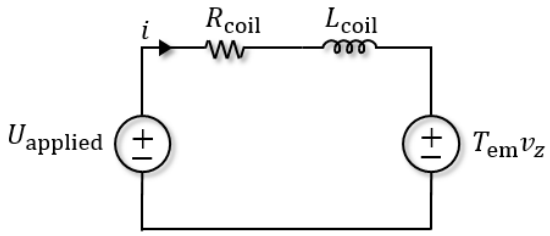

Figure 3. Lumped model for the electrical part of the balanced armature loudspeaker. The used circuit parameters are U_{applied} = 1 V, R_{coil} = 0.5 Ω, L_{coil} = 9 μH, and T_{em} = 0.05 Tm. The unknown v_z is the z-component of the armature velocity, which provides a feedback from the mechanics.

The loudspeaker is connected with a long tube to a 2cc coupler (see Figure 4), which corresponds to a typical measurement setup. The complete thermoacoustics formulation given by Eqs. (1-3) and (8) is used to solve for p, $\mathbf{u}$, and T in both the rear and front volume of the loudspeaker. In the vent and long tube, COMSOL's Narrow Region Acoustics formulation for circular ducts is applied. This formulation uses the analytical solution of the thermoacoustics equations for an infinitely long duct to obtain the effective propagation characteristics. Lossless pressure acoustics is only applied in the large 2cc coupler. This part has a diameter of 1.4 cm, which is much larger than the thermoviscous boundary layers even at the lowest frequencies. Pressure acoustics only solves for the acoustic pressure p and thereby requires less computational resources than thermoacoustics. All together, the complete model contains the coupled frequency domain equations of pressure acoustics (including Narrow Region Acoustics), thermoacoustics, solid mechanics and the electrical circuit. The model is solved for frequencies ranging from 10 Hz up to 10 kHz.

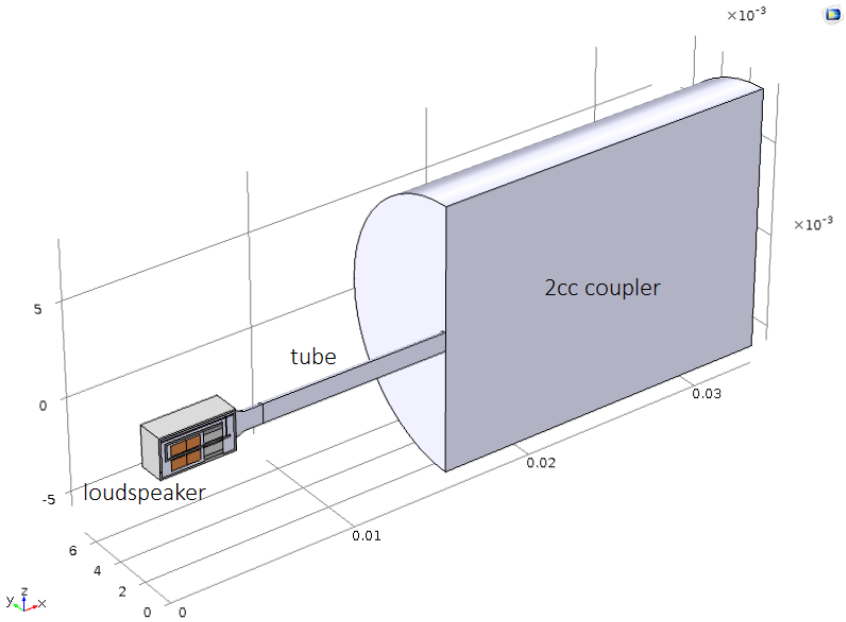

Figure 4. Geometry used in the simulation. A long tube connects the loudspeaker outlet to a 2cc coupler. Due to symmetry in the xz-plane, it is only necessary to solve the problem in one half-space. Geometry dimensions are in meters (note the multiplier 10^{-3} for y- and z-axis).

The calculated sound pressure level (SPL) distribution at 100 Hz is shown in Figure 5(a). It is seen that the SPL is uniform within the rear volume of the receiver, mainly due to the very small dimensions involved. A small gradient in the pressure is observed in the front volume, above the diaphragm. The corresponding displacement fields of the moving parts are shown in Figure 5(b). The displacement is maximal at the edge of the armature, reaching an amplitude of 81 μm. The distribution of the displacement field is qualitatively the same for the whole considered spectral range.

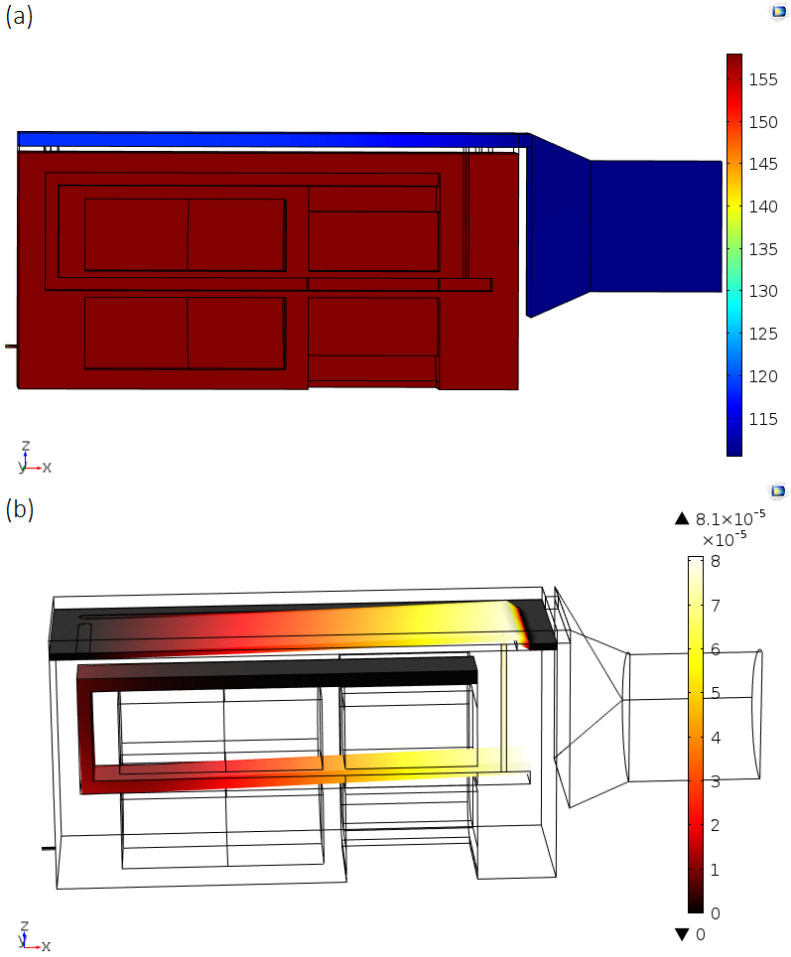

Figure 5. (a) Sound pressure level in the balanced armature loudspeaker operating at 100 Hz. (b) Displacement field of the moving parts in the loudspeaker. The color shows the displacement magnitude in meters.

The sound pressure level at the coupler output is calculated using the standard equation $\mathrm{SPL}_{\mathrm{out}} = 10\log_{10}\left(0.5\left|\frac{p_{\mathrm{ave}}}{20\mu\mathrm{Pa}}\right|^2\right)$, where p_{ave} is the complex amplitude of the pressure, averaged over the output surface of the 2cc coupler. The spectra of the output SPL is shown by the green line in Figure 6. We observe that the SPL is slowly varying up to a frequency of 1 kHz at which the level rises. Note that due to the rather small inductance chosen for the lumped model, the falloff at high frequencies is not visible. In order to study the influence of thermoviscous damping, we also solve the model with lossless pressure acoustics applied everywhere. The resulting SPL at the coupler output is shown by the blue line in Figure 6. A significant difference is observed between the two curves, highlighting the necessity of a thermoacoustics formulation.

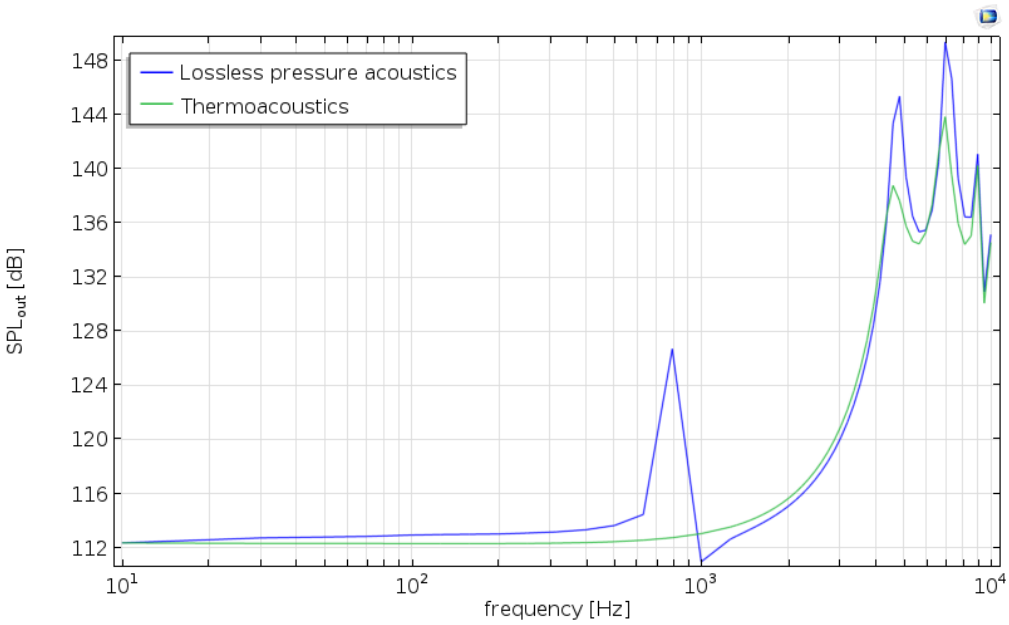

Figure 6. Sound pressure level measured at the coupler output. Thermoviscous damping is taken into account in the front and rear volume (using full thermoacoustics), as well as in the vent and pipe (using narrow region acoustics).

It is also interesting to see in which parts of the setup damping is most pronounced. Therefore, we integrate the thermoviscous power dissipation density over the different parts to calculate the corresponding loss in units of Watts. The obtained spectra are shown in Figure 7. It is seen that at the high frequency peaks, the loss in the front volume and tube are dominant. Only at low frequencies is the damping in the geometrically complex rear volume more important. Note that the thickness of the front volume is only 100 μm, which is on the same order of magnitude as the thermoviscous boundary layer thickness for the higher frequencies. The resonance seen in Figure 6 at 800 Hz is caused by the rear volume's vent. Thermoviscous damping in the vent was verified to completely remove this resonance.

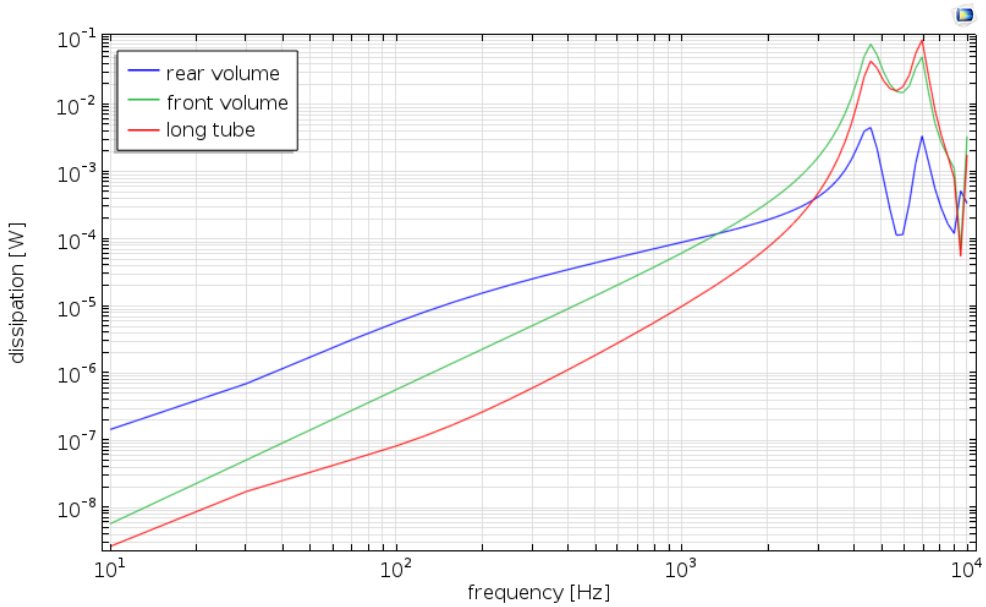

Figure 7. Thermoviscous power dissipation in different parts of the loudspeaker.

The thermoviscous power dissipation density at a frequency of 5100 Hz is shown in Figure 8. This frequency corresponds to the peaks in Figure 7. The boundary layer is clearly visible in the front volume of the loudspeaker, where losses are dominant. The dissipation density is also high in the small vent, but due to its small size, its contribution to the overall loss is insignificant at this frequency. The largest contribution comes from the thin channel that connects the front volume to the sound outlet.

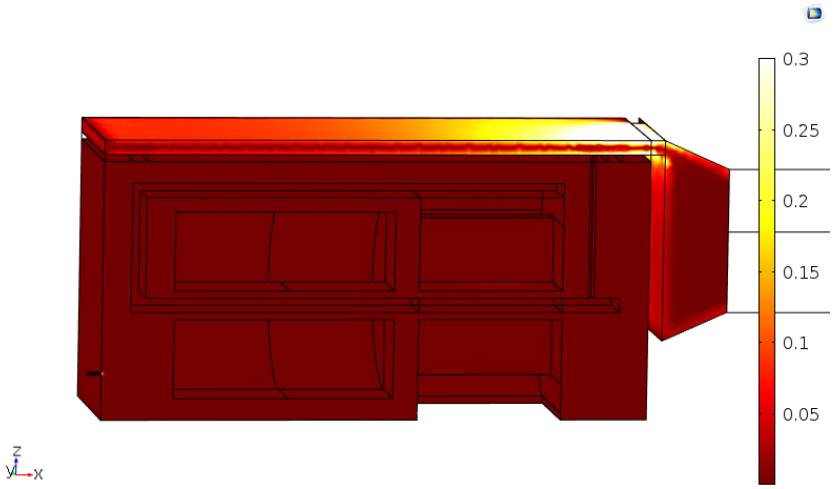

Figure 8. Thermoviscous power dissipation density in the rear and front volume at a frequency of 5100 Hz. The color scale gives the value in units of W/mm^3.

4 CONCLUSIONS

We have shown that when modeling small-scale audio equipment, one should take into account the damping arising from the thermal and viscous boundary layers. Using COMSOL Multiphysics, we have simulated the operation of a balanced armature receiver, for which this damping is present at all audio frequencies. It is seen that a lossless acoustics model is unable to demonstrate accurate results. We also observed that at different frequencies, energy dissipation is localized to different parts of the loudspeaker. Using the presented model, one can optimize and design loudspeakers for improved acoustic performance and energy efficiency.

REFERENCES

[1] Nisula J, Holm J, Mäkivirta A, “Calculating Sound Radiation from Loudspeaker Enclosures Using the Finite Element Analysis”, AES 51st International Conference (2013), #4-1.

[2] Backman J, “Refinements of Transmission Line Loudspeaker Models”, AES Convention 122 (2007), #7071.

[3] Bai M R, You B-C, Lo Y-Y, “Electroacoustic analysis, design, and implementation of a small balanced armature speaker”, J. Acoust. Soc. Am. 136 (2014), 2554-2560.

[4] Jensen J, "Nonlinear Distortion Mechanisms and Efficiency of Miniature Balanced-Armature Loudspeakers" (Doctoral dissertation, Technical University of Denmark, 2014).

[5] Farina A, Campanini S, Chiesi L, Amendola A, Ebri L, "Spatial Sound Recording with Dense Microphone Arrays", AES 55th International Conference (2014), #P-10.

[6] Marttila P, Jensen M J H, "A Hybrid Electroacoustic Lumped and Finite Element Model for Modeling Loudspeaker Drivers", AES 51st International Conference (2013), #4-4.

[7] Skov U, Christensen R, "Overview of 2D and 3D Linear and Non-Linear Electromagnetic, Structural, Vibroacoustic and Viscothermal Finite Element Analysis Simulations on Transducers and Cabinets", AES 51st International Conference (2013), #4-2.

[8] Hedges M J D, Lam Y, "Accuracy of Fully Coupled Loudspeaker Simulation Using COMSOL", Proc. COMSOL Conf., Milan (2009).

[9] Bernhard H, Stieger C, Perriard Y, "New Implantable Hearing Device Based on a Micro-Actuator that is Directly Coupled to the Inner Ear Fluid", Conf. Proc. IEEE Eng. Med. Biol. Soc. (2006), 3162-3165.

[10] Killion M C, "Hearing Aid Transducers", Encyclopedia of Acoustics, Volume 4, Chap. 166, edited by Crocker M J, Wiley, 2007.